

Securing the Sustainability of Global Medical Nuclear Supply Chains Through Economic Cost Recovery, Risk Management, and Optimization

Anna Nagurney

Department of Finance and Operations Management
Isenberg School of Management
University of Massachusetts
Amherst, Massachusetts 01003

Ladimer S. Nagurney

Department of Electrical and Computer Engineering
University of Hartford
West Hartford, CT 06117

Dong Li

Department of Finance and Operations Management
Isenberg School of Management
University of Massachusetts
Amherst, Massachusetts 01003

February 2011

Abstract: In this paper, we develop a new generalized network model for the optimization of the complex operations of medical nuclear supply chains in the case of the radioisotope molybdenum, with a focus on minimizing the total operational cost, the total waste cost, and the risk associated with this highly time-sensitive and perishable, but critical, product used in healthcare diagnostics. Our model allows for the evaluation of transitioning the production and processing of the radioisotope from highly enriched uranium targets to low enriched uranium targets. A case study for North America demonstrates how our model and computational framework can be applied in practice.

Keywords: Supply chains, Nuclear medicine, Sustainable transportation, Healthcare security, Multicriteria decision-making, Risk management, Optimization, Variational inequalities, Generalized networks, Molybdenum, Time-sensitive products, Radioactive decay

1. Introduction

Each day, 41,000 nuclear medical procedures are performed in the United States using Technetium-99m, a radioisotope obtained from the decay of Molybdenum-99. The Molybdenum is produced by primarily irradiating Highly Enriched Uranium (HEU) targets in research reactors. For over two decades, no irradiation and subsequent Molybdenum processing has occurred in the United States. All of the Molybdenum necessary for US-based nuclear medical diagnostic procedures, which include diagnostics for two of the greatest killers, cancer and cardiac problems, comes from foreign sources. Since Molybdenum-99 has a half-life of only 66.7 hours, continuous production is needed to provide the supply for the medical procedures. Thus, the US is critically vulnerable to Molybdenum supply chain disruptions that could significantly affect our healthcare security.

Currently, approximately 60% of the supply of Molybdenum-99 (^{99}Mo) needed for medical procedures in the United States comes from a Canadian reactor, with the remainder coming from Western Europe, with its production taking place in Western Europe, the former Eastern-Bloc States, and South Africa. Worldwide, there are only 9 reactors used for the target irradiation and 6 major processing plants. The shutdown of any of the reactors or processing plants, due to routine maintenance, upgrades, or, as occurred during 2009 and 2010, for emergency repairs, could significantly disrupt the Molybdenum supply and impact medical facilities' abilities to perform the necessary imaging for cardiac and cancer diagnoses (see Ponsard (2010)). Moreover, the number of processors that supply the global market is only four, and they are located in Canada, Belgium, The Netherlands, and South Africa.

Additional challenges to the ^{99}Mo supply chain lie in the reality that limitations in processing capabilities restrict the ability to produce the medical radioisotopes from regional reactors since long-distance transportation of the product during staged in the supply chain raises safety and security risks, and also results in greater decay of the product. The number of generator manufacturers, which place the radioisotopes into containers known as generators, which are directly used by hospitals and imaging facilities, with substantial processing capabilities, is under a dozen (OECD Nuclear Energy Agency (2010b)). In addition, since the majority of the reactors are between 40 and 50 years old, several of the reactors currently used, including the Canadian one, are due to be retired by the end of this decade(Seeverens

(2010) and OECD Nuclear Energy Agency (2010a)).

We now briefly provide some additional background on medical nuclear technology for the convenience of the reader. A radioactive isotope is bound to a pharmaceutical that is injected into the patient and travels to the site or organ of interest in order to construct an image for medical diagnostic purposes. The gamma rays emitted by the radioactive decay of the isotope are then used to construct an image of that site or organ (Berger, Goldsmith, and Lewis (2004)). Technetium, ^{99m}Tc , which is a decay product of Molybdenum-99, ^{99}Mo , is the most commonly used medical radioisotope, used in more than 80% of the radioisotope injections, with more than 30 million procedures worldwide each year. Over 100,000 hospitals in the world use radioisotopes (World Nuclear Association (2011)). In 2008, 18.5 million doses of ^{99m}Tc were injected in the US with 2/3 of them used for cardiac exams, with the other uses including bone scans (Lantheur Medical Imaging, Inc (2009)). By using medical radioisotope techniques, health professionals can enable the earlier and more accurate detection of cardiac problems as well as cancer, the two most common causes of death (see Kochanek et al. (2011)). According to Kahn (2008), the global market for medical isotopes is 3.7 billion US\$ per year.

However, the technology and policy landscape is now changing for medical nuclear supply chains. Although most of the current production of ^{99}Mo uses HEU targets, all producing countries, where economically and technologically feasible, have agreed, in principle, to convert to low enriched uranium (LEU) according to the latest OECD Nuclear Energy Agency (2011) report. However, as noted therein, although the use of LEU targets for ^{99}Mo production has advantages over HEU, with proliferation resistance (and, hence, enhanced global security) being a primary one, along with easier availability of the target material and also easier compliance for its transportation and processing, the negatives, nonetheless, include: a lower production yield than HEU and a greater number of targets needed to be irradiated with associated increased volumes of waste. Indeed, according to Kramer (2011), the South African Nuclear Energy Corp (Necsa) believes that the LEU production process will approximately double the amount of waste generated in extracting the radioisotope, whereas other producers are likely to see a factor of four increase in their wastes. Hence, both production and processing pressures are raised as well as waste management issues.

Since ^{99}Mo decays with a 66.7 hour half-life, approximately 99.9% of the atoms decay in 27.5 days, making its production, transportation, and processing all extremely time-sensitive. In fact, the production of ^{99}Mo is quantified in *Six-day curies end of processing* denoting the activity of the sample 6 days after it was irradiated to highlight this (see OECD Nuclear Energy Agency (2010a)). In addition to the time-sensitivity, the irradiated targets are highly radioactive, significantly constraining HEU target transportation options between the reactor and the processing facilities to only trucks that can transport the heavily shielded transportation containers. While the extracted bulk ^{99}Mo continues to be constrained by its decay, its shielding requirements are reduced, allowing for transportation by multiple modes, including by air (cf. de Lange (2010)). LEU targets, however, can be transported by plane opening up an alternative transportation option to that of trucks, with implications for the medical nuclear supply chain.

A proper model of this critical medical nuclear supply chain, which allows for appropriate economic cost quantification, heavily emphasized by policy-makers (see OECD Nuclear Energy Agency (2011)), must include the physics-based principles of the underlying radioactivity, and must incorporate multicriteria decision-making and optimization to capture the operational and waste management costs as well as risk management, subject to constraints of demand satisfaction at the hospitals and medical facilities. Moreover, the model must be sufficiently flexible and robust in order to provide rigorous solutions as the technological landscape changes.

With the creation of such a sustainable medical nuclear supply chain network economic optimization model, decision-makers, policy-makers, as well as, healthcare providers, would have the ability to analyze the medical nuclear supply chain vulnerabilities and synergies (cf. Nagurney and Qiang (2009)), as well as to explore the relevant costs and risks. In addition, the effects on costs and risks of changes in demand, which is expected to increase given the aging population, could be assessed. Moreover, the various stakeholders including the government, the medical firms, and the hospital and imaging facilities, through such a supply chain network economic optimization model, could determine the true costs of operating the reactors, and the same holds for the processing facilities, as well as the generator manufacturing facilities. Such a transparent framework would enhance healthcare security, would allow for more accurate pricing and cost recovery, and would enable the evaluation of

disruptions to the medical nuclear supply chain.

In Section 2, we develop the multitiered supply chain network economic optimization model for Molybdenum, ^{99}Mo , and describe the various tiers of the supply chain network, consisting of the nuclear reactors, the processors, the generator manufacturing facilities, and, finally, the hospitals and medical facilities, where the medical radioisotopes are injected in the patients. We model the supply chain network optimization problem as a multicriteria system-optimization problem on a generalized network. We identify the specific losses on the links/arcs through the use of the time decay of the radioisotope and we capture distinctions between LEU versus HEU target irradiation and processing. We consider total cost minimization associated with the operational costs, along with the waste management costs, since we are dealing with nuclear products, and the associated risk of the various supply chain network activities which is especially relevant here since these are hazardous products and by-products. Medical nuclear waste management issues have not received much attention in recent reports (cf. OECD Nuclear Energy Agency (2010a,b)). The model's solution provides the optimal levels of production, transportation, and processing of the medical radioisotope, given the demands at the various hospitals and medical imaging facilities.

It is important to emphasize that emerging global and domestic concerns for human health, safety, and the environment are driving organizations to consider not only profits but also their environmental and social responsibilities (Gillett (1993), Cruz (2009), Cruz and Matsypura (2009), Nagurney and Nagurney (2010), and Nagurney and Woolley (2010)). Such issues are also paramount in the case of supply chains that involve the production, transportation, and disposal of hazardous materials, whether as primary products or as by-products, as is the case of medical nuclear supply chains.

Recent work that is relevant to supply chain optimization of other hazardous materials can be categorized as follows: capacity planning, facility location, or routing and scheduling (see Erkut, Tjandra, and Verter (2007)). Most of the studies apply integer programming (see also, e.g., Kara and Verter (2004), Carotenuto, Giordani, and Ricciardeli (2005), and Erkut and Alp (2006), Caramia, Giordani and Iovanella (2010)), stochastic programming (see, e.g., Erkut and Ingolfsson (2005)) or simulation (see, e.g., van der Vorst et al. (2000)) as the methodology of choice. In addition, although risk minimization has been taken into

account in the hazmat transportation literature in addition to cost minimization (see, e.g., Batta and Chiu (1988), List and Mirchandani (1991), Revelle, Cohon, and Shobrys (1991), Marianov and ReVelle (1998), Iakovou et al. (1999), Huang and Cheu (2004), and Erkut and Gzara (2008)), to the authors' knowledge, this important issue has not yet been considered in models of medical nuclear supply chain optimization.

In this paper, in contrast to those referenced above, we develop a system-optimization model for medical nuclear supply chain networks, the objective function of which is the minimization of the total cost and the weighted total risk. Cost and risk are associated with the various processes in the medical nuclear supply chain. Following Alp (1995), we define risk as a measure of the probability and the severity of harm to exposed receptors due to the release and disposal of the associated materials. In the processes of manufacturing and of distribution/storage, the risk functions are concentrated on the quantity of the medical nuclear product, which is captured by the link flow; in transportation/shipment, the risk functions depend on the travel time and the accident probabilities, which are also realized by the link flows and are coupled with the transportation modes. The evidence is as follows.

In the processes of manufacturing and distribution/storage, risks are associated with the production and the disposal of hazmat. Although no risk assessment functions are well-established and widely applied in the literature of medical nuclear transportation, various risk functions have been presented to estimate the risk in the literature of hazmat transportation. The risk here refers to the total risk. Traditional risk functions estimate the risk as the product of the probability or the conditional probability of an accident happening and its consequences (see, e.g., Abkowitz, Eiger, and Srinivasan (1984), Abkowitz and Cheng (1988), Erkut and Verter (1998), Sherali et al. (1997), Jonkmana et al. (2003), Erkut and Ingolfsson (2005), Carotenuto, Giordani, and Ricciardeli (2005), Erkut, Tjandra, and Verter (2007), and Caramia, Giordani and Iovanella (2010)), in which the total probability of an accident happening on a road segment is the product of the unit probability, road length and travel time (in the case of land-based transportation); the consequence of an accident is estimated by the number of shipments, the population exposure, and the area of the impact zone. Based on this traditional function, there is also a literature using risk preference to measure the impact consequences (see, e.g., Abkowitz et al. (1992)). It is widely accepted that the accident probabilities and the incident rates of using different transportation modes are

distinguishing features (Kloeber et al. (1979) and PHSA (Pipeline and Hazardous Materials Safety Administration (2011))). Thus, it is reasonable to assume that, in the case of hazmat transportation, the risk functions depend on the mode of transportation and on the link flows. Of course, it is also true that human factors and subjects play roles in the safety of the total system (Kloeber et al. (1979) and Andersson (1994)), an aspect that should not be ignored.

We use a variational inequality formulation since such a formulation results in an elegant computational procedure. Moreover, the theory of variational inequalities has been applied to a plethora of supply chain modeling, analysis, and design problems (see Nagurney, Dong, and Zhang (2002), Zhang (2006), Nagurney (2006, 2010), Nagurney, Liu, and Woolley (2007), Qiang, Nagurney, and Dong (2009), Nagurney and Nagurney (2010), Liu and Nagurney (2011), and Cruz and Liu (2011)). In addition, variational inequalities have been used to model generalized network applications ranging from spatial price equilibrium problems (see Nagurney and Aronson (1989)) to blood supply chains (cf. Nagurney, Masoumi, and Yu (2012)) and oligopolistic pharmaceutical supply chains (Masoumi, Yu, and Nagurney (2011)). Furthermore, a variational inequality framework provides a rigorous mathematical and computational setting to enable the exploration of alternative economic behaviors among the medical nuclear supply chain stakeholders, including competition (see Nagurney (2006)).

Such a modeling approach is in concert with recent studies that have focused on the security and reliability of medical nuclear supply chains that also emphasize that governments ultimately have the responsibility for establishing an environment conducive to investment in such supply chains (cf. OECD Nuclear Energy Agency (2010a) and Nagurney and Nagurney (2011)). However, to the best of our knowledge, our model is the first general quantitative one to include the engineering, economic, and physics aspects of medical nuclear products with a focus on sustainable operations, cost recovery, and risk management. Indeed, the model captures the economic aspects of the medical nuclear supply chain network, which is an important issue since it has been recognized that usually governments run the reactors, which are research reactors, and the prices associated with the radioisotope may fail to capture the associated costs and, as a consequence, the pricing may be below marginal costs resulting in market failure (see OECD Nuclear Energy Agency (2010a) and Seeverens (2010)).

In earlier work, we focused on the design and redesign of medical nuclear supply chains (see Nagurney and Nagurney (2011)). In that paper, the emphasis was on the long term since construction of the associated facilities, whether research reactors, generator production facilities, or processing facilities, may take some time and may be quite costly. Here, in contrast, our goal is to determine the true economic costs associated with this critical medical nuclear supply chain so as to optimize existing processes. We also focus on HEU versus LEU trade-offs in terms of waste and risk.

In Section 3, we propose a computational approach, which resolves the medical nuclear supply chain network optimization problem into subproblems that can be solved explicitly and exactly at each iteration. In Section 4, we apply the methodology to compute solutions to a realistic medical nuclear supply chain case study, based on North America. In Section 5, we summarize our findings, present our conclusions, and provide suggestions for future research.

2. The Economic Cost Recovery Sustainable Medical Nuclear Supply Chain Network Optimization Model

In this Section, we develop the economic cost recovery sustainable medical nuclear supply chain network optimization model, with a focus on ^{99}Mo , referred to, henceforth, as Mo . We note that the construction is also relevant, with minor modifications, to other radioisotopes, including Iodine-131.

Figure 1 depicts the network topology of the medical nuclear supply chain. The network topology reflects the medical nuclear supply chain at the state of evaluation. Note that the topology is different from the medical nuclear supply chain network topology considered in Nagurney and Nagurney (2011) since therein the focus was on the design from scratch (or redesign) of an existing supply chain network.

In the network, the top level (origin) node 0 represents the organization and the bottom level nodes represent the destination nodes. Every other node in the network denotes a component/facility in the medical nuclear system. A path connecting the origin node to a destination node, corresponding to a demand point, consists of a sequence of directed links which correspond to the supply chain network activities that guarantee that the nuclear product is produced, processed, and, ultimately, distributed to the hospitals and medical imaging facilities, where it is administered to the patients. It is assumed that there exists at least one path joining node 0 with each destination node: $H_1^2, \dots, H_{n_H}^2$.

The solution of the model yields the optimal flows of the medical nuclear product, at minimum total cost and risk.

In the network in Figure 1, there are n_R reactor sites, which produce the radioisotope. These are usually government research reactors and constitute the second tier of nodes of the network: R_1, R_2, \dots, R_{n_R} . The first set of links, connecting the origin node to the second tier, corresponds to the process of radioisotope production. As noted in the Introduction, different reactors irradiate different targets, that is, either HEU or LEU and, hence, the reactors are irradiation target-specific.

The next set of nodes, located in the third tier, consists of the radioisotope processing centers. There exist n_C of these facilities, denoted, respectively, by $C_1^1, C_2^1, \dots, C_{n_C}^1$, to

which the Mo is shipped after being produced at the reactor sites. Thus, the next set of links connecting tiers two and three of the network topology represents the transportation of the radioisotope. Transportation at this stage of the radioisotope, which is a hazardous material, in the case of HEU irradiated targets (as opposed to LEU ones) is done solely by a single mode of transportation, that is, by truck using specialized containers. This single mode of transportation is represented by single links joining the pairs of nodes. Hence, the HEU processing facilities must be located fairly near to the reactors and the transportation is done by land. However, cf. Figure 1, in the case of LEU targets, either truck or air transport (or both) may be feasible.

At the processing centers, the Mo is extracted and purified. Note that, as depicted by the supply chain network topology, not every processing facility can process both LEU and HEU irradiated targets, but some may be able to and we consider such a case study in Section 4. Consequently, in the network in Figure 1, the first processor only processes the type of target produced by the first reactor, and so on. This processing is represented by the links emanating from the nodes: $C_1^1, C_2^1, \dots, C_{n_C}^1$ and ending in the nodes: $C_1^2, C_2^2, \dots, C_{n_C}^2$, with the latter set of nodes being the fourth tier nodes. The last processor in the Figure is an LEU processor and, hence, there are multiple transportation options, depicted accordingly by multiple links.

Figure 1 can be adapted/modified as the technology landscape in terms of transitioning from HEU to LEU processing occurs.

The fifth tier of the network is associated with the generator manufacturing facilities, and these nodes are joined with the fourth tier nodes by links which represent the multiple modes of transportation that are available for transporting the purified Mo to the generator manufacturing facilities. The number of generator manufacturing facilities is given by n_G . These facilities are denoted by $G_1^1, \dots, G_{n_G}^1$, respectively, and need not be located near the processing facilities.

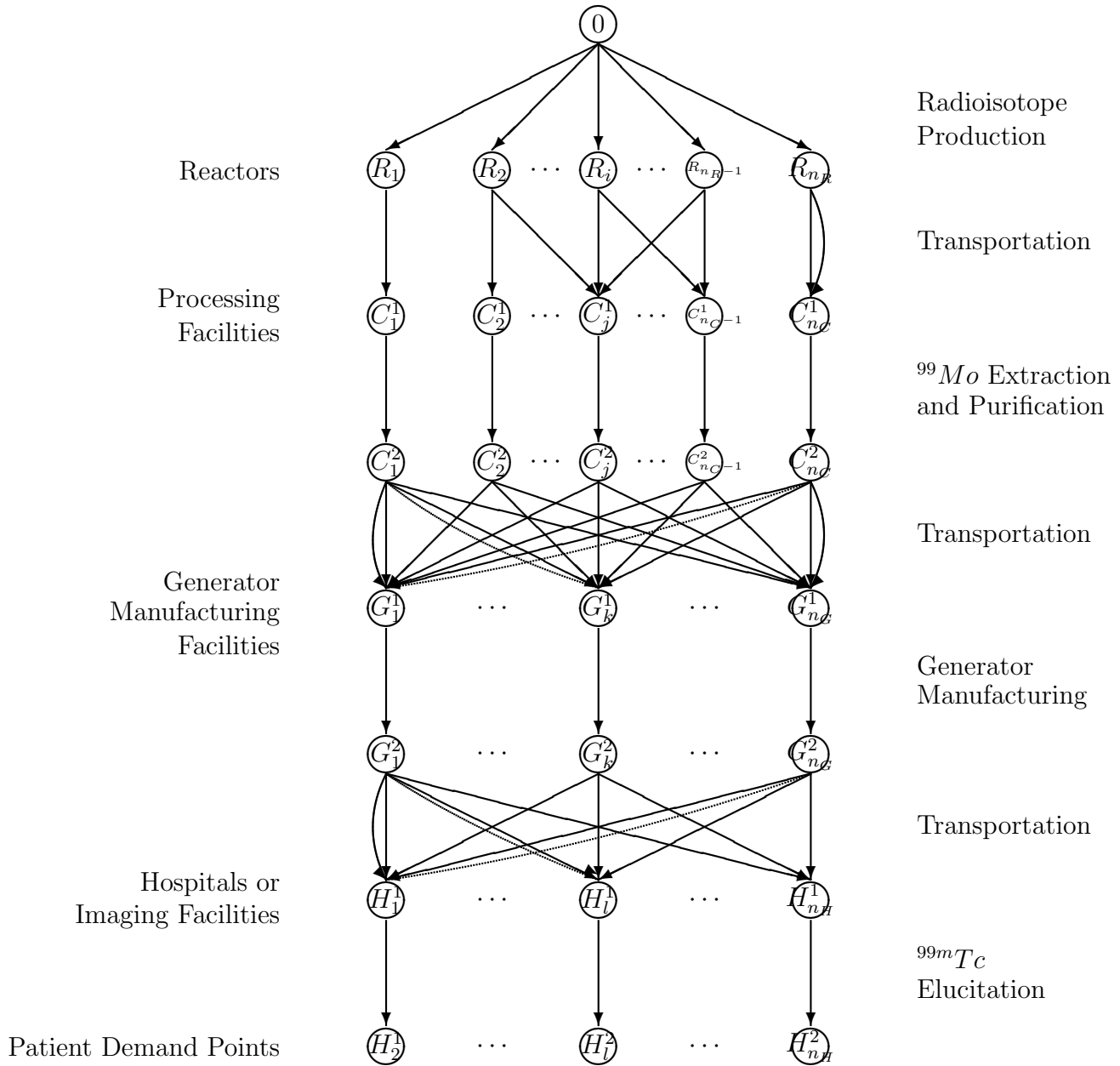


Figure 1: The Medical Nuclear Supply Chain Network Topology

At the generator manufacturing facilities the radioisotope is processed and packaged to be used at the medical facilities. The links that emanate from the generator manufacturing facility nodes terminate in the sixth tier set of nodes, respectively, denoted by $G_1^2, \dots, G_{n_G}^2$ in Figure 1, which represent the completion of this stage of processing.

From the latter generator nodes, there emanate transportation links and these links, as the preceding transportation links, correspond to multiple modes of transportation, as appropriate, including not only trucking but also, for example, common carrier air transportation. These links terminate in the seventh tier of nodes, $H_1^1, \dots, H_{n_H}^1$, which represent the hospitals and the medical facilities that dispense the radioisotope to the patients. There is still one more stage of processing, producing the final injectible radioisotope that is represented by the final set of links in Figure 1 and terminating in nodes: $H_1^2, \dots, H_{n_H}^2$, which represent the final patient demand points.

The medical nuclear supply chain network topology, as depicted in Figure 1, is denoted by $\mathcal{G} = [N, L]$, where N and L denote the sets of nodes and links, respectively.

The formalism that we use is that of multicriteria system-optimization, since the organization wishes to determine at what level the reactors should operate; the same for the processing centers, and the generator manufacturers. Furthermore, the organization seeks to minimize the total risk, because the product of concern is a hazardous one, as well as the total costs associated with the production, processing, and transportation activities, as well as the total cost of discarding the nuclear waste product associated with each of the links.

We assume that the demands must be satisfied since we are dealing with a healthcare product and the medical procedures must be scheduled in advance.

With each link of the network, we associate a unit operational cost function that reflects the cost of operating that particular medical nuclear supply chain activity. The links are denoted by a, b , etc. The unit operational cost on link a is denoted by c_a and is a function of flow on that link, f_a . The *total* operational cost on link a is denoted by \hat{c}_a , and is constructed as:

$$\hat{c}_a(f_a) = f_a \times c_a(f_a), \quad \forall a \in L. \quad (1)$$

The link total cost functions are assumed to be convex and continuously differentiable.

The origin/destination (O/D) nodes are the pairs of nodes: $(0, H_k^2)$; $k = 1, \dots, n_H$. Let \mathcal{P}_k denote the set of paths, which represent the alternative associated possible supply chain network processes, joining $(0, H_k^2)$. \mathcal{P} denotes the set of all paths joining node 0 to the destination nodes, and $n_{\mathcal{P}}$ denotes the number of paths.

Let d_k denote the demand for the radioisotope at the demand point H_k^2 ; $k = 1, \dots, n_H$.

As in Nagurney and Nagurney (2011), we associate with every link a in the network, a multiplier α_a , which corresponds to the percentage of decay and additional loss over that link. This multiplier lies in the range $(0,1]$, for the network activities, where $\alpha_a = 1$ means that 100% of the initial flow on link a reaches the successor node of that link, reflecting that there is no decay/waste/loss on link a . The multiplier α_a can be modeled as the product of two terms, a radioactive decay multiplier α_{da} and a processing loss multiplier $\alpha_{\iota a}$.

The Underlying Physics and the Link and Path Multipliers

For completeness and easy reference, we now outline the underlying physics of radioactive decay in this application, along with how we handle it through arc and path multipliers. The activity of a radioisotope (in disintegrations per unit time) is proportional to the quantity of that isotope, i.e.,

$$\frac{dN}{dt} \propto N, \quad (2)$$

where $N = N(t)$ = the quantity of a radioisotope. The quantity of a radioisotope in a time interval t is then given by

$$N(t) = N_0 e^{-\lambda t}, \quad (3)$$

where N_0 is the quantity present at the beginning of the interval and λ is the decay constant of the radioisotope (see Berger, Goldsmith, and Lewis (2004)).

We can represent the radioactive decay multiplier α_{da} for link a as

$$\alpha_{da} = e^{-\lambda t_a}, \quad (4)$$

where t_a is the time spent on link a . The decay constant, λ , in turn, can be conveniently

represented by an experimentally measured value, called the half-life $t_{1/2}$, where

$$t_{1/2} = \frac{\ln 2}{\lambda}. \quad (5)$$

The values of the half-lives of radioisotopes are tabulated in the American Institute of Physics (1972). Hence, we can write α_{da} as

$$\alpha_{da} = e^{-\lambda t_a} = e^{-\ln 2 \frac{t_a}{t_{1/2}}} = 2^{-\frac{t_a}{t_{1/2}}}. \quad (6)$$

The value of $t_{1/2}$ for Mo , as noted in the Introduction, is 66.7 hours.

The processing loss multiplier α_{la} for link a is a factor in the range $(0,1]$ that quantifies for the losses that occur during processing. Different processing links may have different values for this parameter. For transportation links, however, there is no loss beyond that due to radioactive decay; therefore, $\alpha_{la} = 1$ for such links. For the top-most manufacturing links $\alpha_a = 1$.

As mentioned earlier, f_a denotes the (initial) flow on link a . Let f'_a denote the final flow on that link; i.e., the flow that reaches the successor node of the link. Therefore,

$$f'_a = \alpha_a f_a, \quad \forall a \in L. \quad (7)$$

The organization is also responsible for disposing the hazardous waste.

Since α_a is constant, and known apriori, a total discarding cost function, \hat{z}_a , can be defined accordingly, which is a function of the flow, f_a , and is assumed to be convex and continuously differentiable and given by:

$$\hat{z}_a = \hat{z}_a(f_a), \quad \forall a \in L. \quad (8)$$

Note that, in processing/producing an amount of radioisotope f_a , one knows from the physics the amount of hazardous waste and, hence, a discarding function of the form (8) is appropriate. As noted in the Introduction, LEU target processing can generate several times the amount of waste that HEU target processing does (Kramer (2011)).

Let x_p represent the (initial) flow of Mo on path p joining the origin node with a destination node. The path flows must be nonnegative, that is,

$$x_p \geq 0, \quad \forall p \in \mathcal{P}, \quad (9)$$

since the nuclear product will be produced, processed, transported, etc., in nonnegative quantities.

Let μ_p denote the multiplier corresponding to the loss on path p , which is defined as the product of all link multipliers on links comprising that path, that is,

$$\mu_p \equiv \prod_{a \in p} \alpha_a, \quad \forall p \in \mathcal{P}. \quad (10)$$

The demand at demand point R_k , d_k , is the sum of all the final flows on paths joining $(0, H_k^2)$:

$$d_k \equiv \sum_{p \in \mathcal{P}_k} \mu_p x_p, \quad k = 1, \dots, n_H. \quad (11)$$

Indeed, although the amount of radioisotope that originates on a path p is x_p , the amount (due to radioactive decay, etc.) that actually arrives at the destination (terminal node) of this path is $x_p \mu_p$.

The multiplier α_{ap} is the product of the multipliers of the links on path p that precede link a in that path. This multiplier can be expressed as:

$$\alpha_{ap} \equiv \begin{cases} \delta_{ap} \prod_{a' < a} \alpha_{a'}, & \text{if } \{a' < a\} \neq \emptyset, \\ \delta_{ap}, & \text{if } \{a' < a\} = \emptyset, \end{cases} \quad (12)$$

where $\{a' < a\}$ denotes the set of the links preceding link a in path p , and δ_{ap} is defined as equal to one if link a is contained in path p ; otherwise, it is equal to zero, and \emptyset denotes the null set. In other words, α_{ap} is equal to the product of all link multipliers preceding link a in path p . If link a is not contained in path p , then α_{ap} is set to zero. The relationship between the link flow, f_a , and the path flows is as follows:

$$f_a = \sum_{p \in \mathcal{P}} x_p \alpha_{ap}, \quad \forall a \in L. \quad (13)$$

The total cost minimization objective faced by the organization includes the total cost of operating the various links and the total discarding cost of waste/loss over the links. This

optimization problem can be expressed as:

$$\text{Minimize } \sum_{a \in L} \hat{c}_a(f_a) + \sum_{a \in L} \hat{z}_a(f_a) \quad (14)$$

subject to: constraints (9), (11), and (13), and

$$f_a \leq \bar{u}_a, \quad \forall a \in L. \quad (15)$$

Constraint (15) guarantees that the flow on a link cannot exceed the capacity on that link.

As mentioned earlier, the minimization of total costs is not the only objective. A major challenge for a medical nuclear organization is to capture the risk associated with different activities in the nuclear supply chain network. Unlike the demand, which can be projected according to the scheduling of medical procedures, albeit with some uncertainty involved, there is risk associated with the production, processing, and transportation of nuclear medical radioisotopes.

Let \hat{r}_a denote the total risk on link $a \in L$. Based on our review of the literature discussed in the Introduction, we assume that the total risk on a link is denoted by a risk function that is a function of the flow on the link, that is,

$$\hat{r}_a = \hat{r}_a(f_a), \quad \forall a \in L. \quad (16)$$

We assume that the total risk functions are convex and continuously differentiable.

For example, for a transportation link a , the total risk function would measure the impact of the travel time, the population density that the transportation route goes through, the unit probability of an accident using the particular mode represented by the link, the area of the impact zone, the length of the link, etc., and, ideally, also include impact of human factors. In the case of a non-transportation processing link, the function would capture analogous aspects but with a focus on the specific processing activity.

The organization attempts to minimize the total risk over all links.

Thus, the risk minimization objective function for the organization can be expressed as:

$$\text{Minimize } \sum_{a \in L} \hat{r}_a(f_a). \quad (17)$$

The Multicriteria Decision-Making Problems in Link Flows and in Path Flows

The supply chain network optimization problem for a medical nuclear product can be expressed as a multicriteria decision-making problem. The organization seeks to determine the optimal levels of radioisotope processed on each supply chain network link subject to the minimization of the total cost (operational and discarding) as well as the minimization of the total risk. The weight associated with the total cost objective (14) serves as the numeraire, and is set equal to 1. On the other hand, a weight of ω is assigned by the decision-maker to the total risk objective (17) and it can be interpreted as the factor of risk aversion. ω can also be interpreted as a risk to cost conversion factor.

Thus, the multicriteria optimization problem is:

$$\text{Minimize } \sum_{a \in L} \hat{c}_a(f_a) + \sum_{a \in L} \hat{z}_a(f_a) + \omega \sum_{a \in L} \hat{r}_a(f_a) \quad (18)$$

subject to: constraints: (9), (11), (13), and (15).

The above optimization problem is in terms of link flows. It can also be expressed in terms of path flows:

$$\text{Minimize } \sum_{p \in \mathcal{P}} (\hat{C}_p(x) + \hat{Z}_p(x)) + \omega \sum_{p \in \mathcal{P}} \hat{R}_p(x) \quad (19)$$

subject to: constraints (9), (11), and (15), where the path total operational cost function, $\hat{C}_p(x)$, the path total discarding cost function, $\hat{Z}_p(x)$, and the path total risk function, $\hat{R}_p(x)$ are, respectively, derived from $C_p(x)$, $Z_p(x)$, and $R_p(x)$ as follows:

$$\hat{C}_p(x) = x_p \times C_p(x), \quad \hat{Z}_p(x) = x_p \times Z_p(x), \quad \hat{R}_p(x) = x_p \times R_p(x), \quad \forall p \in \mathcal{P}, \quad (20)$$

with the unit cost functions on path p , i.e., $C_p(x)$, $Z_p(x)$, and $R_p(x)$, in turn, defined as below:

$$C_p(x) \equiv \sum_{a \in L} c_a(f_a) \alpha_{ap}, \quad Z_p(x) \equiv \sum_{a \in L} z_a(f_a) \alpha_{ap}, \quad R_p(x) \equiv \sum_{a \in L} r_a(f_a) \alpha_{ap}, \quad \forall p \in \mathcal{P}. \quad (21)$$

We associate the Lagrange multiplier γ_a with constraint (15) for each link a , and we denote the optimal Lagrange multiplier by $\gamma_a^*, \forall a \in L$. The Lagrange multipliers may be interpreted as shadow prices. We group these Lagrange multipliers into the vector γ .

Let K denote the feasible set such that:

$$K \equiv \{(x, \gamma) | x \in R_+^{n_p}, (11) \text{ and } (15) \text{ hold}, \gamma \in R_+^{n_L}\}. \quad (22)$$

Before stating the variational inequality formulation of the problem, we recall a lemma, due to Nagurney, Amasoumi, and Yu (2012). This lemma was derived for another time-sensitive product supply chain in healthcare – that of human blood. However, in that application the arc and path multipliers have an entirely different meaning than that in the case of medical nuclear products.

Lemma

The partial derivatives of the total operational cost, the total discarding cost, and the total risk (cf. (19)) with respect to a path flow are, respectively, given by:

$$\begin{aligned} \frac{\partial(\sum_{q \in \mathcal{P}} \hat{C}_q(x))}{\partial x_p} &\equiv \sum_{a \in L} \frac{\partial \hat{c}_a(f_a)}{\partial f_a} \alpha_{ap}, \quad \forall p \in \mathcal{P}, \\ \frac{\partial(\sum_{q \in \mathcal{P}} \hat{Z}_q(x))}{\partial x_p} &\equiv \sum_{a \in L} \frac{\partial \hat{z}_a(f_a)}{\partial f_a} \alpha_{ap}, \quad \forall p \in \mathcal{P}, \\ \frac{\partial(\sum_{q \in \mathcal{P}} \hat{R}_q(x))}{\partial x_p} &\equiv \sum_{a \in L} \frac{\partial \hat{r}_a(f_a)}{\partial f_a} \alpha_{ap}, \quad \forall p \in \mathcal{P}. \end{aligned} \quad (23)$$

Proof: See Nagurney, Masoumi, and Yu (2012).

We now derive the variational inequality formulations of the problem in terms of path flows and link flows.

Theorem: Variational Inequality Formulations

The optimization problem (19), subject to its constraints, is equivalent to the variational inequality problem: determine the vector of optimal path flows and the vector of optimal Lagrange multipliers $(x^*, \gamma^*) \in K$, such that:

$$\begin{aligned} \sum_{k=1}^{n_R} \sum_{p \in \mathcal{P}_k} \left[\frac{\partial(\sum_{q \in \mathcal{P}} \hat{C}_q(x^*))}{\partial x_p} + \frac{\partial(\sum_{q \in \mathcal{P}} \hat{Z}_q(x^*))}{\partial x_p} + \sum_{a \in L} \gamma_a^* \delta_{ap} + \omega \frac{\partial(\sum_{q \in \mathcal{P}} \hat{R}_q(x^*))}{\partial x_p} \right] \times [x_p - x_p^*] \\ + \sum_{a \in L} \left[\bar{u}_a - \sum_{p \in \mathcal{P}} x_p^* \alpha_{ap} \right] \times [\gamma_a - \gamma_a^*] \geq 0, \quad \forall (x, \gamma) \in K. \end{aligned} \quad (24)$$

Variational inequality (24), in turn, can be rewritten in terms of link flows as: determine the vector of optimal link flows and the vector of optimal Lagrange multipliers $(f^*, \gamma^*) \in K^1$, such that:

$$\begin{aligned} \sum_{a \in L} \left[\frac{\partial \hat{c}_a(f_a^*)}{\partial f_a} + \frac{\partial \hat{z}_a(f_a^*)}{\partial f_a} + \gamma_a^* + \omega \frac{\partial \hat{r}_a(f_a^*)}{\partial f_a} \right] \times [f_a - f_a^*] \\ + \sum_{a \in L} [\bar{u}_a - f_a^*] \times [\gamma_a - \gamma_a^*] \geq 0, \quad \forall (f, \gamma) \in K^1, \end{aligned} \quad (25)$$

where K^1 denotes the feasible set:

$$K^1 \equiv \{(f, \gamma) | \exists x \geq 0, (9), (11), (13), \text{ and } (15) \text{ hold, and } \gamma \geq 0\}. \quad (26)$$

Proof: First, we prove the result for path flows (cf. (24)).

The convexity of \hat{C}_p , \hat{Z}_p , and \hat{R}_p for all paths p holds since \hat{c}_a , \hat{z}_a , and \hat{r}_a were assumed to be convex for all links a .

Since the objective function (19) is convex and the feasible set K is closed and convex, the variational inequality (24) follows from the standard theory of variational inequalities (see Nagurney (1999)).

As for the proof of the variational inequality (25), now that (24) is established, we can apply the equivalence between partial derivatives of total costs on paths and partial derivatives of total costs on links from Lemma 1. Also, using (13) and (15), we can rewrite the

formulation in terms of link flows rather than path flows. Thus, the second part of Theorem 1, that is, the variational inequality in link flows (25), also holds.

Variational inequality (24) can be put into standard form VI (F, \mathcal{K}) (see Nagurney (1999)) as follows: determine $X^* \in \mathcal{K}$ such that:

$$\langle F(X^*)^T, X - X^* \rangle \geq 0, \quad \forall X \in \mathcal{K}, \quad (27)$$

where $\langle \cdot, \cdot \rangle$ denotes the inner product in n -dimensional Euclidean space, if we define the feasible set $\mathcal{K} \equiv K$, and the column vector $X \equiv (x, \gamma)$, and $F(X) \equiv (F_1(X), F_2(X))$, where:

$$F_1(X) = \left[\frac{\partial(\sum_{q \in \mathcal{P}} \hat{C}_q(x))}{\partial x_p} + \frac{\partial(\sum_{q \in \mathcal{P}} \hat{Z}_q(x))}{\partial x_p} + \sum_{a \in L} \gamma_a \delta_{ap} + \omega \frac{\partial(\sum_{q \in \mathcal{P}} \hat{R}_q(x))}{\partial x_p}; \quad p \in \mathcal{P} \right],$$

$$F_2(X) = \left[\bar{u}_a - \sum_{p \in \mathcal{P}} x_p \alpha_{ap}; \quad a \in L \right]. \quad (28)$$

We will utilize variational inequality (24) in path flows for the proposed computational approach and numerical case study.

3. The Computational Approach

In this Section, we provide the computational approach for the solution of medical nuclear supply chain network design problems in practice.

Specifically, we propose the modified projection method (Korpelevich (1977)), but in path flows, rather than in link flows (see, e.g., Nagurney and Qiang (2009) Liu and Nagurney (2011), and references therein). This algorithm, in the context of our new model, yields subproblems that can be solved exactly, and in closed form, for the path flows, using a variant of the exact equilibration algorithm, adapted to incorporate arc/path multipliers, along with explicit formulae for the Lagrange multipliers.

The modified projection is guaranteed to converge if the function F that enters the variational inequality satisfies monotonicity and Lipschitz continuity (see Nagurney (1999)).

We now recall the modified projection method, where \mathcal{T} denotes an iteration counter.

Step 0: Initialization

Set $X^0 \in \mathcal{K}$. Let $\mathcal{T} = 1$ and let η be a scalar such that $0 < \eta \leq \frac{1}{L}$, where L is the Lipschitz continuity constant.

Step 1: Computation

Compute $\tilde{X}^{\mathcal{T}}$ by solving the VI subproblem:

$$\langle \tilde{X}^{\mathcal{T}} + \eta F(X^{\mathcal{T}-1}) - X^{\mathcal{T}-1}, X - \tilde{X}^{\mathcal{T}} \rangle \geq 0, \quad \forall X \in \mathcal{K}. \quad (29)$$

Step 2: Adaptation

Compute $X^{\mathcal{T}}$ by solving the VI subproblem:

$$\langle X^{\mathcal{T}} + \eta F(\tilde{X}^{\mathcal{T}}) - X^{\mathcal{T}-1}, X - X^{\mathcal{T}} \rangle \geq 0, \quad \forall X \in \mathcal{K}. \quad (30)$$

Step 3: Convergence Verification

If $\max |X_l^{\mathcal{T}} - X_l^{\mathcal{T}-1}| \leq \epsilon$, for all l , with $\epsilon > 0$, a prespecified tolerance, then stop; else, set $\mathcal{T} =: \mathcal{T} + 1$, and go to Step 1.

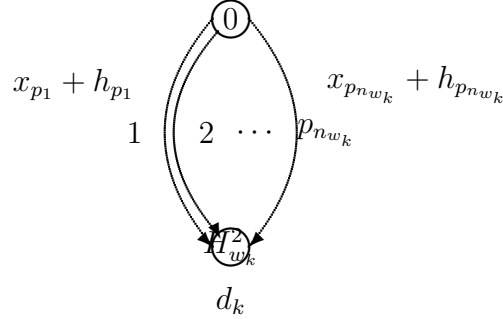


Figure 2: Special Network Structure of an Induced Path Flow Subproblem for Each Demand Point k

The VI subproblems in (29) and (30) are quadratic programming problems with special structure that result in straightforward computations. Explicit formulae for (29) for the medical nuclear supply chain network problem are now given for the Lagrange multipliers. Analogous formulae for (30) can then be easily obtained. Subsequently, we follow up with how the path flow values in (29) can be determined (a similar approach can then be used to determine the path flows for (30)).

Explicit Formulae for the Lagrange Multipliers at Step 1 (cf. (29))

$$\tilde{\gamma}_a^{\mathcal{T}} = \max\{0, \gamma_a^{\mathcal{T}-1} + \eta(\sum_{p \in \mathcal{P}} x_p^{\mathcal{T}-1} \delta_{ap} - \bar{u}_a)\}, \quad \forall a \in L. \quad (31)$$

Recall that the feasible set \mathcal{K} , in terms of the path flows, requires that the path flows be nonnegative and that the demand constraint (11) holds for each demand point. The induced path flow subproblems in (29) and (30), hence, have a special network structure of the form given in Figure 2.

Specifically, the path flow subproblems that one must solve in Step 1 (see (29)) (we have suppressed the iteration superscripts below) have the following form for each demand point

$k; k = 1, \dots, n_H:$

$$\text{Minimize } \frac{1}{2} \sum_{p \in \mathcal{P}_k} x_p^2 + \sum_{p \in \mathcal{P}_k} h_p x_p \quad (32)$$

subject to:

$$d_k \equiv \sum_{p \in \mathcal{P}_k} \mu_p x_p, \quad (33)$$

$$x_p \geq 0, \quad \forall p \in \mathcal{P}_k, \quad (34)$$

where $h_p \equiv x_p^{T-1} - \eta \left[\frac{\partial(\sum_{q \in \mathcal{P}} \hat{C}_q(x^{T-1}))}{\partial x_p} + \frac{\partial(\sum_{q \in \mathcal{P}} \hat{Z}_q(x^{T-1}))}{\partial x_p} + \sum_{a \in L} \gamma_a^{T-1} \delta_{ap} + \omega \frac{\partial(\sum_{q \in \mathcal{P}} \hat{R}_q(x^{T-1}))}{\partial x_p} \right]$.

We now present an exact equilibration algorithm, adapted to handle the multipliers, which can be applied to compute the solution to problem (32) for each demand point, subject to constraints (33) and (34). An analogous set of subproblems in path flows can be set up and solved accordingly for Step 2 (cf. (30)). For further background on such algorithms, see Dafermos and Sparrow (1969) and Nagurney and Qiang (2009).

An Exact Equilibration Algorithm for a Generalized Specially Structured Network

Step 0: Sort

Sort the fixed terms $\frac{h_p}{\mu_p}; p \in \mathcal{P}_k$ in nondescending order and relabel the paths/links accordingly. Assume, from this point on, that they are relabeled. Set $r = 1$.

Step 1: Computation

Compute

$$\lambda_{w_k}^r = \frac{\sum_{i=1}^r \mu_{p_i} h_{p_i} + d_k}{\sum_{i=1}^r \mu_{p_i}^2}. \quad (35)$$

Step 2: Evaluation

If $\frac{h_{p_r}}{\mu_{p_r}} < \lambda_k^r \leq \frac{h_{p_{r+1}}}{\mu_{p_{r+1}}}$, then stop; set $s = r$ and go to Step 3; otherwise, let $r = r + 1$ and return to Step 1. If $r = n_k$, where n_k denotes the number of paths connecting destination node H_k^2 with origin node \cdot , then set $s = n_k$ and go to Step 3.

Step 3: Path Flow Determination

Set

$$\begin{aligned}x_{p_i} &= \mu_p \lambda_k^s - h_{p_i}, \quad i = 1, \dots, s. \\x_{p_i} &= 0, \quad i = s + 1, \dots, n_k.\end{aligned}\tag{36}$$

In summary, the proposed computational procedure, at Steps 1 and 2 (see (29) and (30)) induces subproblems of special structure, each of which can be solved explicitly and in closed form. For the induced subproblems in Lagrange multipliers, we have provided the formulae (31), whereas for the induced subproblems in the path flows, we have provided a variant of the exact equilibration algorithm to handle the multipliers.

The modified projection method is guaranteed to converge to a solution of the medical nuclear supply chain network problem provided that the function F (cf. (28)) is monotone and Lipschitz continuous. Monotonicity follows under our imposed assumptions and Lipschitz continuity will also hold provided that the marginal total cost and marginal risk functions have bounded second order partial derivatives.

4. The Case Study

In this section, we describe a case study. We consider the medical nuclear supply chain network depicted in Figure 3. In particular, we consider the Molybdenum-99 supply chain in North America including the existing Canadian reactor, NRU, the Canadian processing facility located in Ottawa, AECL-MDS Nordion, and the two US generator manufacturing facilities. This reactor and processing facility are likely to be decommissioned around 2016. The NRU reactor is located in Chalk River, Ontario and uses HEU targets. Transportation of the irradiated targets from NRU to AECL - MDS Nordion takes place by truck. There are two generator manufacturers in the United States (and none in Canada) located in Billerica, Massachusetts and outside of St. Louis, Missouri.

In addition, in our case study, we have included another potential source of irradiated targets, as discussed in Kramer (2011), Canada's TRIUMF linear accelerator located in Vancouver, British Columbia. Molybdenum irradiated from LEU targets at TRIUMF is expected in 2012. Hence, we are interested in optimizing the operations of this medical nuclear supply chain scenario. During the transition from HEU targets to LEU the Nordion processing facility will be able to process both HEU and LEU targets, as depicted in Figure 3. Hence, each of these target processing stages has its own processing link (cf. links 3 and 24 in Figure 3). There are also expected to be available two modes of transportation from TRIUMF to Nordion, truck and air transport, as depicted by two associated alternative transportation links (22, 23) in Figure 3.

Links 4, 6, 9, 11, 13, 14, 16, 17, and 23 correspond to transportation by air, whereas links 2, 5, 10, 12, 15, and 22 correspond to transportation by truck. The capacities on the links were obtained from OECD (2010b, 2011) and Kramer (2011). The transportation links are assumed not to be capacity limited (that is, we assume very large capacities), which we denote by *large* in Table 1. In the computations, we set the value to 5,000,000 for all such links. We implemented the modified projection method, along with the generalized exact equilibration algorithm, as described in Section 3, for the solution of our medical nuclear supply chain network case study. The ϵ in the convergence criterion was 10^{-6} . The algorithm was implemented in FORTRAN and a Unix-based system at the University of Massachusetts was used for the computations.

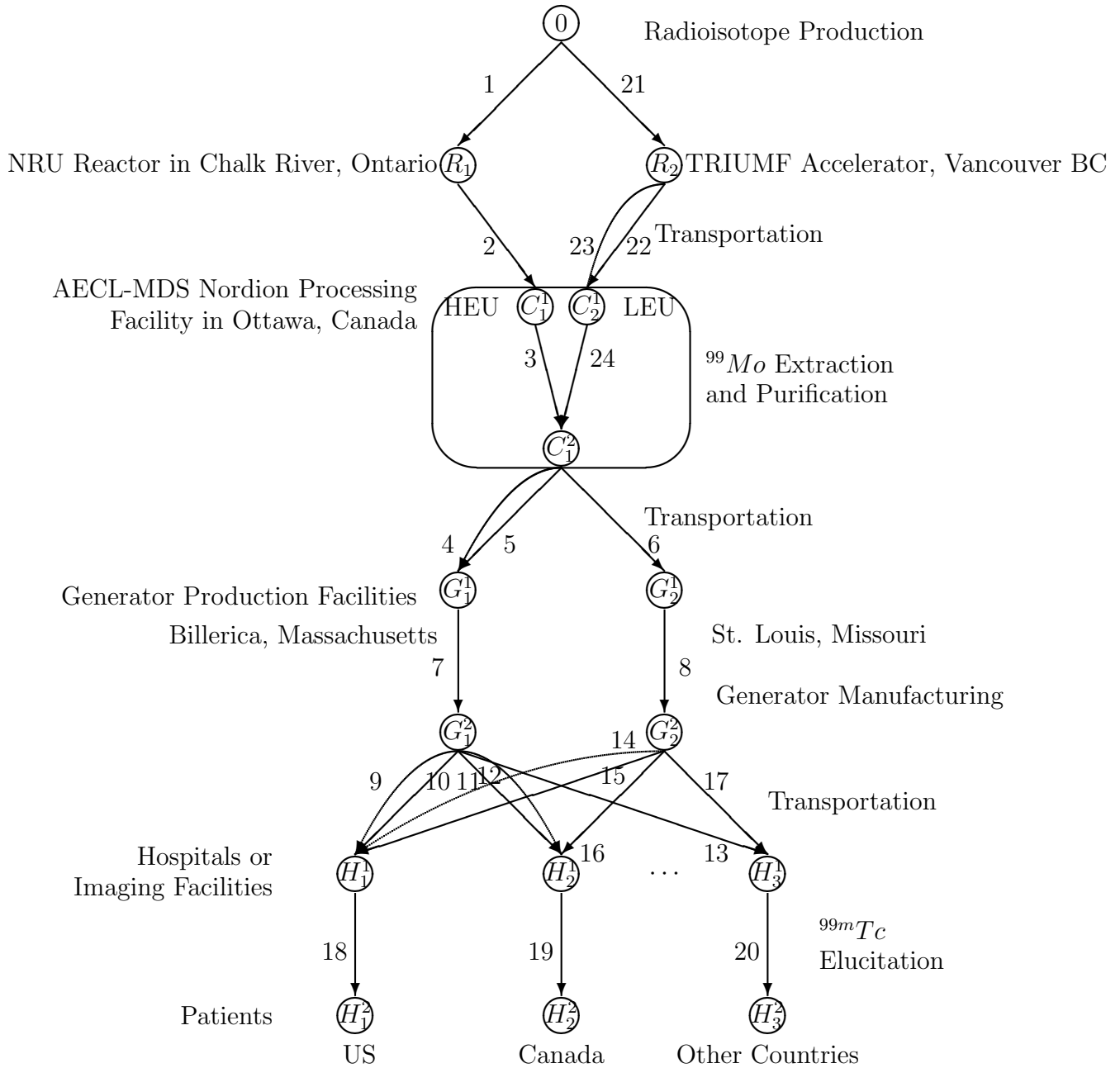


Figure 3: The Medical Nuclear Supply Chain Topology for ^{99}Mo from Canada to the United States, Canada, and Other Countries

We calculated the values of the arc multipliers α_{da} , for all links $a = 1, \dots, 24$, using data in the OECD (2010a) report and in the National Research Council (2009) report, which included the approximate times associated with the various links in the supply chain network in Figure 3. According to OECD (2010a), we may assume that there is no loss a_{la} on each link a for $a = 1, \dots, 24$, except for processing links 3 and 24; hence, $\alpha_{la} = 1$ for all the former links; therefore, $\alpha_a = \alpha_{da}$ for all those links, as reported in Table 1. In the case of links 3 and 24, $\alpha_{la} = .8$ and $\alpha_{da} = .883$; therefore, $\alpha_3 = \alpha_{24} = .706$. All flows (and capacities) are reported in Curies.

Operating cost data were taken from OECD (2010b) and converted to per Curie processed or generated. As noted by the National Research Council (2009), the US generator prices are proprietary, but could be estimated from a functional form derived from publicly available prices for Australian generators coupled with several spot prices for US made generators.

The risk functions for transportation links were estimated based upon the overall accident rate per kilometer for aircraft and trucks carrying nuclear material as reported in Resnikoff (1992). These were converted to a per Curie basis using an average distance traveled and the approximate number of Curies transported per week. The functions for risk for shipment of bulk ^{99}Mo and irradiated targets were increased by 1 and 2 orders of magnitude, respectively, to account for the increased severity of an accident during this stage. The risk during generator elucitation was assumed to be similar to air transport of a generator ($\approx 2 \times 10^{-6} f_x$). Risks during generator production, bulk ^{99}Mo extraction, and irradiation were assumed to be 1, 2, and 3 orders of magnitude greater, respectively.

We assumed three demand points corresponding, respectively, to the collective demands in the US, in Canada, and in other countries (such as Mexico and the Caribbean Islands). We are using 3 demand points, as approximations, in order to be able to report the input and output data for transparency purposes. The demands were as follows: $d_1 = 3,600$, $d_2 = 1,800$, and $d_3 = 1,000$ and these denote the demands, in Curies, per week. These values were obtained by using the daily number of procedures in the US and extrapolating for the others. The units for the link flows are also Curies.

The arc multipliers, the total operational cost functions, the total discarding cost functions, the total risk functions, and the optimal link flow and Lagrange multiplier solutions

are reported in Table 1.

The weight ω was set equal to 1 in Example 1. Note that this weight can also represent a conversion factor of risk to cost.

As can be seen from the results in Table 1, none of the links were operated at full capacity and, hence, all the Lagrange multipliers were equal to 0.00. Note also that the transportation links: 10, 12, 15, 16, and 22 have zero flow. Hence, not only does cost efficiency play a role but also the perishability of the product. Transport by truck may be cheaper, but it takes longer, and, hence, there may be less product available once the shipment is delivered. Note that the LEU processing link 24 had positive flow and air transport (given the distance) was used (see flow on link 23) to deliver the LEU targets to the processing facility. This makes sense, given the time-sensitivity and perishability of molybdenum, and the distance between the Vancouver accelerator and the processing facility in Ottawa. Also, it is interesting to observe, as speculated by Kramer (2011), that the new LEU production facility (cf. link 21) is expected to produce about 30% of the needs, and this was also the result obtained in our computation. The HEU reactor in Chalk River (cf. link 1) produced 9720.70 Curies whereas the Vancouver one produced 5867.24 Curies (cf. link 21).

The value of the objective function (cf. (18)) was: 2,096,149,888.00 whereas the total risk (cf. (17)) was: 4,060.81.

It is also important to emphasize that the demand was met at the demand points but, given the perishability of the radioisotope, many more Curies had to be produced (as well as processed).

We then proceeded to construct Example 2 (see the data in Table 2) and we raised the evaluation of the weight ω from 1 to 1000. The remainder of the input data were as in Table 1. The computed optimal solution for Example 2 is also reported in Table 2.

Table 1: Link Multipliers, Link Total Operational Cost, Total Discarding Cost, Total Risk Functions, Link Capacity, and Optimal Link Flow and Lagrange Multiplier Solution for the Case Study Example 1

Link a	α_a	$\hat{c}_a(f_a)$	$\hat{z}_a(f_a)$	$\hat{r}_a(f_a)$	\bar{u}_a	f_a^*	λ_a^*
1	1.00	$2f_1^2 + 25.6f_1$	0.00	$2.00 \times 10^{-2}f_1$	33,353	9720.20	0.00
2	.969	$f_2^2 + 5f_2$	0.00	$3.18 \times 10^{-1}f_2$	<i>large</i>	9720.20	0.00
3	.706	$5f_3^2 + 192f_3$	$5f_3^2 + 80f_3$	$2.00 \times 10^{-3}f_3$	32,154	9419.35	0.00
4	.920	$2f_4^2 + 4f_4$	0.00	$1.59 \times 10^{-1}f_4$	<i>large</i>	3045.90	0.00
5	.901	$f_5^2 + f_5$	0.00	$2.16 \times 10^{-3}f_5$	<i>large</i>	2327.34	0.00
6	.915	$f_6^2 + 2f_6$	0.00	$6.9 \times 10^{-3}f_6$	<i>large</i>	4934.45	0.00
7	.804	$f_7^2 + 166f_7$	$2f_7^2 + 7f_7$	$2.00 \times 10^{-4}f_7$	19,981	4899.16	0.00
8	.804	$f_8^2 + 166f_8$	$2f_7^2 + 7f_7$	$2.00 \times 10^{-4}f_8$	19,981	4515.02	0.00
9	.883	$2f_9^2 + 4f_9$	0.00	$2.00 \times 10^{-4}f_9$	<i>large</i>	1623.06	0.00
10	.779	$f_{10}^2 + 1f_{10}$	0.00	$1.47 \times 10^{-2}f_{10}$	<i>large</i>	0.00	0.00
11	.883	$2f_{11}^2 + 4f_{11}$	0.00	$2.00 \times 10^{-4}f_{11}$	<i>large</i>	2038.51	0.00
12	.688	$f_{12}^2 + 2f_{12}$	0.00	$1.47 \times 10^{-2}f_{12}$	<i>large</i>	0.00	0.00
13	.688	$2.5f_{13}^2 + 2f_{13}$	0.00	$1.98 \times 10^{-4}f_{13}$	<i>large</i>	277.36	0.00
14	.883	$2f_{14}^2 + 2f_{14}$	0.00	$7.33 \times 10^{-3}f_{14}$	<i>large</i>	2453.95	0.00
15	.779	$f_{15}^2 + 7f_{15}$	0.00	$1.00 \times 10^{-4}f_{15}$	<i>large</i>	0.00	0.00
16	.688	$2f_{16}^2 + 4f_{16}$	0.00	$1.00 \times 10^{-4}f_{16}$	<i>large</i>	0.00	0.00
17	.688	$2f_{17}^2 + 6f_{17}$	0.00	$1.98 \times 10^{-5}f_{17}$	<i>large</i>	1176.13	0.00
18	1.00	$2f_{18}^2 + 800f_{18}$	$4f_{18}^2 + 80f_{18}$	$2.00 \times 10^{-5}f_{18}$	5,000	3600.00	0.00
19	1.00	$f_{19}^2 + 600f_{19}$	$1f_{19}^2 + 60f_{19}$	$2.00 \times 10^{-5}f_{19}$	3,000	1800.00	0.00
20	1.00	$f_{20}^2 + 300f_{20}$	$1f_{20}^2 + 30f_{20}$	$2.00 \times 10^{-5}f_{20}$	2,000	1000.00	0.00
21	1.00	$4f_{21}^2 + 50f_{21}$	0.00	$2.00 \times 10^{-2}f_{21}$	10,006	5867.24	0.00
22	.436	$6f_{22}^2 + 6f_{22}$	0.00	$1.04 \times 10^1f_{22}$	<i>large</i>	0.00	0.00
23	.883	$3f_{23}^2 + 21f_{23}$	0.00	$1.44 \times 10^{-2}f_{23}$	<i>large</i>	5867.24	0.00
24	.706	$5f_{24}^2 + 192f_{24}$	$10f_{24}^2 + 160f_{24}$	$2.00 \times 10^{-3}f_{24}$	10,006	5180.77	0.00

As can be seen from Table 2, the same links as in Example 1 had zero flows. The value of the objective function was now: 2,100,204,416.00 and the total risk was now: 4,055.70. The risk was reduced, as expected, since ω was increased. Note, for example, that the link flows shifted from links with higher total risk to those with lower total risk, such as the shift from link 1 to link 21. However, the total value of the objective function increased due to the higher value of ω .

We then constructed Example 3. The data were as for Example 2 but now we considered a medical nuclear supply chain disruption in the form of a capacity reduction at the NRU reactor with its capacity being reduced to 9000. The complete input and output data are reported in Table 3. Note that since the capacity at link 1 was reached, there was a positive associated Lagrange multiplier on that link.

The value of the objective function was now: 2,117,958,400.00 and the total risk was: 3865.07. Interestingly, this was the lowest value obtained in the three examples. For this example, the total risk decreased even more significantly than that observed in Example 2 relative to Example 1.

As the capacity associated with link 1 decreased, in order to satisfy the demands and minimize the costs (and losses), the link flows shifted to links with higher capacities and larger arc multipliers, such as the shift from link 1 to 21, and the shift from link 5 to link 4, although link 4 was the one with higher total cost.

Table 2: Link Multipliers, Link Total Operational Cost, Total Discarding Cost, Total Risk Functions, Link Capacity, and Optimal Link Flow and Lagrange Multiplier Solution for the Case Study Example 2

Link a	α_a	$\hat{c}_a(f_a)$	$\hat{z}_a(f_a)$	$\hat{r}_a(f_a)$	\bar{u}_a	f_a^*	λ_a^*
1	1.00	$2f_1^2 + 25.6f_1$	0.00	$2.00 \times 10^{-2}f_1$	33,353	9716.86	0.00
2	.969	$f_2^2 + 5f_2$	0.00	$3.18 \times 10^{-1}f_2$	<i>large</i>	9716.86	0.00
3	.706	$5f_3^2 + 192f_3$	$5f_3^2 + 80f_3$	$2.00 \times 10^{-3}f_3$	32,154	9415.64	0.00
4	.920	$2f_4^2 + 4f_4$	0.00	$1.59 \times 10^{-1}f_4$	<i>large</i>	3020.34	0.00
5	.901	$f_5^2 + f_5$	0.00	$2.16 \times 10^{-3}f_5$	<i>large</i>	2350.27	0.00
6	.915	$f_6^2 + 2f_6$	0.00	$6.9 \times 10^{-3}f_6$	<i>large</i>	4937.57	0.00
7	.804	$f_7^2 + 166f_7$	$2f_7^2 + 7f_7$	$2.00 \times 10^{-4}f_7$	19,981	4896.31	0.00
8	.804	$f_8^2 + 166f_8$	$2f_7^2 + 7f_7$	$2.00 \times 10^{-4}f_8$	19,981	4517.88	0.00
9	.883	$2f_9^2 + 4f_9$	0.00	$2.00 \times 10^{-4}f_9$	<i>large</i>	1622.27	0.00
10	.779	$f_{10}^2 + 1f_{10}$	0.00	$1.47 \times 10^{-2}f_{10}$	<i>large</i>	0.00	0.00
11	.883	$2f_{11}^2 + 4f_{11}$	0.00	$2.00 \times 10^{-4}f_{11}$	<i>large</i>	2038.51	0.00
12	.688	$f_{12}^2 + 2f_{12}$	0.00	$1.47 \times 10^{-2}f_{12}$	<i>large</i>	0.00	0.00
13	.688	$2.5f_{13}^2 + 2f_{13}$	0.00	$1.98 \times 10^{-4}f_{13}$	<i>large</i>	275.86	0.00
14	.883	$2f_{14}^2 + 2f_{14}$	0.00	$7.33 \times 10^{-3}f_{14}$	<i>large</i>	2454.74	0.00
15	.779	$f_{15}^2 + 7f_{15}$	0.00	$1.00 \times 10^{-4}f_{15}$	<i>large</i>	0.00	0.00
16	.688	$2f_{16}^2 + 4f_{16}$	0.00	$1.00 \times 10^{-4}f_{16}$	<i>large</i>	0.00	0.00
17	.688	$2f_{17}^2 + 6f_{17}$	0.00	$1.98 \times 10^{-5}f_{17}$	<i>large</i>	1177.63	0.00
18	1.00	$2f_{18}^2 + 800f_{18}$	$4f_{18}^2 + 80f_{18}$	$2.00 \times 10^{-5}f_{18}$	5,000	3600.00	0.00
19	1.00	$f_{19}^2 + 600f_{19}$	$1f_{19}^2 + 60f_{19}$	$2.00 \times 10^{-5}f_{19}$	3,000	1800.00	0.00
20	1.00	$f_{20}^2 + 300f_{20}$	$1f_{20}^2 + 30f_{20}$	$2.00 \times 10^{-5}f_{20}$	2,000	1000.00	0.00
21	1.00	$4f_{21}^2 + 50f_{21}$	0.00	$2.00 \times 10^{-2}f_{21}$	10,006	5872.24	0.00
22	.436	$6f_{22}^2 + 6f_{22}$	0.00	$1.04 \times 10^1f_{22}$	<i>large</i>	0.00	0.00
23	.883	$3f_{23}^2 + 21f_{23}$	0.00	$1.44 \times 10^{-2}f_{23}$	<i>large</i>	5872.24	0.00
24	.706	$5f_{24}^2 + 192f_{24}$	$10f_{24}^2 + 160f_{24}$	$2.00 \times 10^{-3}f_{24}$	10,006	5185.19	0.00

Table 3: Link Multipliers, Link Total Operational Cost, Total Discarding Cost, Total Risk Functions, Link Capacity, and Optimal Link Flow and Lagrange Multiplier Solution for the Case Study Example 3

Link a	α_a	$\hat{c}_a(f_a)$	$\hat{z}_a(f_a)$	$\hat{r}_a(f_a)$	\bar{u}_a	f_a^*	λ_a^*
1	1.00	$2f_1^2 + 25.6f_1$	0.00	$2.00 \times 10^{-2}f_1$	9000.00	9000.00	49667.88
2	.969	$f_2^2 + 5f_2$	0.00	$3.18 \times 10^{-1}f_2$	<i>large</i>	9000.00	0.00
3	.706	$5f_3^2 + 192f_3$	$5f_3^2 + 80f_3$	$2.00 \times 10^{-3}f_3$	32,154	8722.89	0.00
4	.920	$2f_4^2 + 4f_4$	0.00	$1.59 \times 10^{-1}f_4$	<i>large</i>	3173.72	0.00
5	.901	$f_5^2 + f_5$	0.00	$2.16 \times 10^{-3}f_5$	<i>large</i>	2168.41	0.00
6	.915	$f_6^2 + 2f_6$	0.00	$6.9 \times 10^{-3}f_6$	<i>large</i>	4962.43	0.00
7	.804	$f_7^2 + 166f_7$	$2f_7^2 + 7f_7$	$2.00 \times 10^{-4}f_7$	19,981	4873.56	0.00
8	.804	$f_8^2 + 166f_8$	$2f_7^2 + 7f_7$	$2.00 \times 10^{-4}f_8$	19,981	4540.62	0.00
9	.883	$2f_9^2 + 4f_9$	0.00	$2.00 \times 10^{-4}f_9$	<i>large</i>	1612.58	0.00
10	.779	$f_{10}^2 + 1f_{10}$	0.00	$1.47 \times 10^{-2}f_{10}$	<i>large</i>	0.00	0.00
11	.883	$2f_{11}^2 + 4f_{11}$	0.00	$2.00 \times 10^{-4}f_{11}$	<i>large</i>	2038.51	0.00
12	.688	$f_{12}^2 + 2f_{12}$	0.00	$1.47 \times 10^{-2}f_{12}$	<i>large</i>	0.00	0.00
13	.688	$2.5f_{13}^2 + 2f_{13}$	0.00	$1.98 \times 10^{-4}f_{13}$	<i>large</i>	267.26	0.00
14	.883	$2f_{14}^2 + 2f_{14}$	0.00	$7.33 \times 10^{-3}f_{14}$	<i>large</i>	2464.43	0.00
15	.779	$f_{15}^2 + 7f_{15}$	0.00	$1.00 \times 10^{-4}f_{15}$	<i>large</i>	0.00	0.00
16	.688	$2f_{16}^2 + 4f_{16}$	0.00	$1.00 \times 10^{-4}f_{16}$	<i>large</i>	0.00	0.00
17	.688	$2f_{17}^2 + 6f_{17}$	0.00	$1.98 \times 10^{-5}f_{17}$	<i>large</i>	1186.23	0.00
18	1.00	$2f_{18}^2 + 800f_{18}$	$4f_{18}^2 + 80f_{18}$	$2.00 \times 10^{-5}f_{18}$	5,000	3600.00	0.00
19	1.00	$f_{19}^2 + 600f_{19}$	$1f_{19}^2 + 60f_{19}$	$2.00 \times 10^{-5}f_{19}$	3,000	1800.00	0.00
20	1.00	$f_{20}^2 + 300f_{20}$	$1f_{20}^2 + 30f_{20}$	$2.00 \times 10^{-5}f_{20}$	2,000	1000.00	0.00
21	1.00	$4f_{21}^2 + 50f_{21}$	0.00	$2.00 \times 10^{-2}f_{21}$	10,006	6650.96	0.00
22	.436	$6f_{22}^2 + 6f_{22}$	0.00	$1.04 \times 10^1f_{22}$	<i>large</i>	0.00	0.00
23	.883	$3f_{23}^2 + 21f_{23}$	0.00	$1.44 \times 10^{-2}f_{23}$	<i>large</i>	6650.96	0.00
24	.706	$5f_{24}^2 + 192f_{24}$	$10f_{24}^2 + 160f_{24}$	$2.00 \times 10^{-3}f_{24}$	10,006	5872.80	0.00

5. Summary and Suggestions for Future Research

In this paper, we developed a new model of sustainable medical nuclear supply chain operations management that incorporates the time-dependent and perishable nature of radioisotopes as well as the hazardous aspects which affect not only the transportation modes but also waste management and risk management issues.

The model is multitiered and incorporates the realities of the technology in this important healthcare sector that is transitioning globally from highly enriched uranium targets to low enriched uranium ones. The model is a generalized network model that includes multicriteria decision-making so that the organization can minimize both total operating and waste management costs as well as the risk associated with the various medical nuclear supply chain network activities of processing, generator production, transportation, and ultimate usage in medical procedures at hospitals and other appropriate medical facilities. Each link has associated with it an arc multiplier which is constructed based on physics principles of radioactive decay of the radioisotope, in this case, molybdenum. Hence, our model traces the amount of the radioisotope that is left as a particular pathway of the supply chain is traversed. Capacities on the links reflect the realities of the production, processing, generation, and transportation activities.

The formulation of the model and the qualitative analysis exploit the theory of variational inequalities since it yields a very elegant procedure for computational purposes. Moreover, it provides us with the foundation to explore other scenarios as the technology landscape continues to evolve and to bring other participants into medical nuclear production.

A numerical case study based on North America, with the focus of an existing HEU reactor and an LEU accelerator that is expected to come online soon, reveals the generality and practicality of our framework.

Acknowledgments

The first author acknowledges support from the John F. Smith Memorial Fund at the University of Massachusetts Amherst.

References

American Institute of Physics Handbook 3rd edition, McGraw Hill, New York, NY, 1972, 8-6 - 8-91.

Abkowitz, M., Cheng, P., 1988. Developing a risk/cost framework for routing truck movements of hazardous materials. *Accident Analysis and Preview*, 20(1), 39-51.

Abkowitz, M., Eiger, A., Srinivasan, S., 1984. Estimating release rates and costs of transporting hazardous waste. In: *Transportation Research Record 977*, TRB, National Research Council, Washington, D.C., 2230.

Abkowitz, M., Lepofsky, M., Cheng, P., 1992. Selecting criteria for designating hazardous materials highway routes. *Transportation Research Record*, 1333, 30-35.

Alp, E., 1995. Risk-based transportation planning practices overall methodology and a case example. *Information Systems and Operational Research*, 33(1), 4-19.

Andersson, S. E., 1994. Safe transport of dangerous goods - road, rail or sea - A screening of technical and administrative factors. *European Journal of Operational Research*, 75(3), 499-507.

Batta, R., Chiu, S. S., 1988. Optimal obvious paths on a network: Transportation of hazardous materials. *Operations Research*, 36(1), 84-92.

Berger, S. A., Goldsmith, W., Lewis, E. R. eds., 2004. *Introduction to Bioengineering*. Oxford University Press, Oxford, UK.

Caramia, M., Giordani, S., Iovanella, A., 2010. On the selection of k routes in multiobjective hazmat route planning. *IMA Journal of Management Mathematics*, 21, 239-251.

Carotenuto, P., Giordani, S., Ricciardeli, S., 2005. Finding minimum and equitable risk routes for hazmat shipments. *Computers and Operations Research*, 34, 1304-1327.

Cruz, J., 2009. The impact of corporate social responsibility in supply chain management: Multicriteria decision-making approach. *Decision Support Systems*, 48(1), 224-236.

- Cruz, J. M., Liu, Z., 2011. Modeling and analysis of multiperiod effects of social relationship on supply chain networks. *European Journal of Operational Research*, 214, 39-52.
- Cruz, J., Matsypura, D., 2009. Supply chain networks with corporate social responsibility through integrated environmental decision-making. *International Journal of Production Research*, 47(3), 621-648.
- Dafermos, S. C., Sparrow, F. T., 1969. The traffic assignment problem for a general network. *Journal of Research of the National Bureau of Standards*, 73B, 91-118.
- de Lange, F., 2010. Covidien's role in the supply chain of Molybdenum-99 and Technetium-99m generators. *tijdschrift voor nucleaire geneeskunde*, 32,593-596.
- Erkut, E., Alp, O., 2006. Integrated routing and scheduling of hazmat trucks with stops en-route. *Transportation Science*, 41(1), 107-122.
- Erkut, E., Gzara, F., 2008. Solving the hazmat transport network design problem. *Computers and Operations Research*, 35, 2234-2247.
- Erkut, E., Ingolfsson, A., 2005. Transport risk models for hazardous materials: Revisited. *Operations Research Letters*, 33, 81-89.
- Erkut, E., Tjandra, S.A., Verter, V., 2007. Transportation. In: *Handbooks in Operations Research and Management Science*, volume 14, Chapter 9, 539-621.
- Erkut, E., Verter, V., 1998. Modeling of transport risk for hazardous materials. *Operations Research*, 46(5), 625-642.
- Gillett, J., 1993. Ensuring suppliers' environmental performance. *Purchasing and Supply Management*, 28-30.
- Huang, B., Cheu, R. L., 2004. GIS and genetic algorithms for hazmat route planning with security considerations. *International Journal of Geographical Information Science*, 18(8), 769-787.
- Iakovou, E., Douligieris C., Lii, H., Ip, C., Yudhbir, L., 1999. A maritime global route

planning model for hazardous materials transportation. *Transportation Science*, 33(1), 34-48.

Jonkmana, S. N., van Gelder, P.H.A.J.M., Vrijling, J. K., 2003. An overview of quantitative risk measures for loss of life and economic damage. *Journal of Hazardous Materials*, A99, 1-30.

Kara, B.Y., Verter, V., 2004. Design a road network for hazardous material transportation. *Transportation Science*, 38 (2), 188-196.

Kloeber, G., Cornell, M., McNamara T., Moscati, A., 1979. Risk assessment of air versus other transportation modes for explosives and flammable cryogenic liquids. Volume I: Risk assessment method and results. Report DOT/RSPA/MTB-79/13, US Department of Transportation.

Kahn, L. H., 2008. The potential dangers in medical isotope production. *Bulletin of the Atomic Scientists*, March 16, <http://thebulletin.org/node/163>.

Kochanek, K. D., Xu, J., Murphy, S. L., Minino, A. M., Kung, H.-C., 2011. Deaths: preliminary data for 2009, *National Vital Statistics Reports*, Vol. 59, No. 4, March 16.

Korpelevich, G.M., 1977. The extragradient method for finding saddle points and other problems. *Matekon*, 13, 35-49.

Kramer, D., 2011. Drive to end civilian use of HEU collides with medical isotope production. *Physics Today*, February, 17-10.

Lantheur Medical Imaging, Inc., 2009. Lantheur Medical Imaging takes proactive steps to mitigate impact of global molybdenum-99 supply chain operations on operations. Press Release, May 20, <http://www.lantheur.com/News-Press-2009-0520.html>.

List, G., Mirchandani, P., 1991. An integrated network planar multiobjective model for routing and siting for hazardous materials and wastes. *Transportation Science*, 25(2), 146-156.

- Liu, Z., Nagurney, A., 2011. Supply chain outsourcing under exchange rate risk and competition. *OMEGA*, 39, 539-549.
- Marianov, V., ReVelle, C., 1998. Linear, non-approximated models for optimal routing in hazardous environments. *The Journal of the Operational Research Society*, 49(2), 157-164.
- Masoumi, A. H., Yu, M., and Nagurney, A., 2011. A supply chain generalized network oligopoly model for pharmaceuticals under brand differentiation and perishability. To appear in *Transportation Research E*.
- Nagurney, A., 1999. *Network Economics: A Variational Inequality Approach*, second and revised edition. Kluwer Academic Publishers, Dordrecht, The Netherlands.
- Nagurney, A., 2006. *Supply Chain Network Economics: Dynamics of Prices, Flows, and Profits*. Edward Elgar Publishing, Cheltenham, England.
- Nagurney, A., 2010. Optimal supply chain network design and redesign at minimal total cost and with demand satisfaction. *International Journal of Production Economics*, 128, 200-208.
- Nagurney, A., Aronson, J., 1989. A general dynamic spatial price network equilibrium model with gains and losses. *Networks*, 19, 751-769.
- Nagurney, A., Dong, J., Zhang, D., 2002. A supply chain network equilibrium model. *Transportation research E*, 38, 281-303.
- Nagurney, A., Liu, Z., Woolley, T., 2007. Sustainable supply chain networks and transportation. *International Journal of Sustainable Transportation*, 1, 29-51.
- Nagurney, A., Masoumi, A., Yu, M., 2012. Supply chain network operations management of a blood banking system with cost and risk minimization. *Computational Management Science*, in press.
- Nagurney, A., Nagurney, L. S., 2010. Sustainable supply chain network design: A multicriteria perspective. *International Journal of Sustainable Engineering*, 3, 189-197.

Nagurney, A., Nagurney, L. S., 2011. Medical nuclear supply chain design: A tractable network model and computational approach. Isenberg School of Management, University of Massachusetts Amherst. Available at:

http://http://supernet.isenberg.umass.edu/articles/Medical_Nuclear_Supply_Chains.pdf

Nagurney, A., Qiang, Q., 2009. Fragile Networks: Identifying Vulnerabilities and Synergies in an Uncertain World. John Wiley & Sons, Hoboken, New Jersey.

Nagurney, A., Woolley, T., 2010. Environmental and cost synergy in supply chain network integration in mergers and acquisitions in sustainable energy and transportation systems. In: Proceedings of the 19th International Conference on Multiple Criteria Decision Making, Lecture Notes in Economics and Mathematical Systems, Ehrgott, M., Naujoks, B., Stewart, T., Wallenius, J., Editors, Springer, Berlin, Germany, pp 51-78.

OECD Nuclear Energy Agency, 2010a. The supply of medical radioisotopes: Interim report of the OECD/NEA high-level group on security of supply of medical radioisotopes.

OECD, 2010b. Nuclear Energy Agency, The supply of medical radioisotopes: An economic study of the molybdenum-99 supply chain.

OECD, 2011. Nuclear Energy Agency, The supply of medical radioisotopes: The path to reliability NEA No. 6985.

PHSA (Pipeline and Hazardous Materials Safety Administration), 2011. Top Consequence Hazardous Materials by Commodities and Failure Modes, 12-13.

Ponsard, B., 2010. Mo-99 supply issues: Report and lessons learned, presented at the 14th International Topical Meeting on the Research Reactor Fuel Management (RRFM 2010), Marrakech, Morocco, 21-25 March, published by the European Nuclear Society, ENS RRFM 2010 Transactions.

Qiang, Q., Nagurney, A., Dong, J., 2009. Modeling of supply chain risk under disruptions with performance measurement and robustness analysis. In Managing Supply Chain Risk and Vulnerability: Tools and Methods for Supply Chain Decision Makers. Wu, T., Blackhurst, J., eds., Springer, Berlin, Germany, pp 91-111.

- Resnikoff, M., 1992. Study of transportation accident severity. Radioactive Waste Management Associates for the Nevada Nuclear Waste Project Office, February.
- ReVelle, C.J., Cohon, J., Shobry, D., 1991. Simultaneous siting and routing in the disposal of hazardous wastes. *Transportation Science*, 25, 138-145.
- Seeverens, H. J. J., 2010. The economics of the molybdenum-99/Technetium-99m supply chain. *tijdschrift voor nucleaire geneeskunde*, 32, 604-608.
- Sherali, H. D., Brizendine, L. D., Glickman, T. S., Subramanian, S., 1997. Low probability-high consequence considerations in routing hazardous material shipments. *Transportation Science*, 31(3), 237-251.
- van der Vorst, J.G.A.J., Beulens, A.J.M. and van Beek, P., 2000. Modelling and simulating multi-echelon food systems. *European Journal of Operations Research*, 122, 354-366.
- World Nuclear Association Radioisotopes in medicine, 2011. January 26.
<http://www.world-nuclear.org/inf55.html>.
- Zhang, D., 2006. A network economic model for supply chain versus supply chain competition, *OMEGA*, 34, 283-295.